Stochastic Approach to Phonon-Assisted Optical Absorption

Marios Zacharias, Christopher E. Patrick,[*] and Feliciano Giustino[†]

Department of Materials, University of Oxford, Parks Road, Oxford OX1 3PH, United Kingdom
(Received 8 June 2015; published 19 October 2015)

We develop a first-principles theory of phonon-assisted optical absorption in semiconductors and insulators which incorporates the temperature dependence of the electronic structure. We show that the Hall-Bardeen-Blatt theory of indirect optical absorption and the Allen-Heine theory of temperature-dependent band structures can be derived from the present formalism by retaining only one-phonon processes. We demonstrate this method by calculating the optical absorption coefficient of silicon using an importance sampling Monte Carlo scheme, and we obtain temperature-dependent line shapes and band gaps in good agreement with experiment. The present approach opens the way to predictive calculations of the optical properties of solids at finite temperature.

In semiconductors and insulators exhibiting indirect band gaps the optical transitions near the fundamental edge require the absorption or emission of phonons in order to fulfill the crystal momentum selection rule. This mechanism is discussed in every introduction to solid state physics [1,2]. The theory of phonon-assisted indirect optical transitions was developed by Hall, Bardeen, and Blatt (HBB) [3,4], and forms the basis for our current understanding of phonon-assisted optical processes.

Despite the popularity of the HBB theory, only very recently was this formalism combined successfully with first-principles density-functional theory calculations [5] powered by Wannier interpolation [6,7]. The work of Ref. [5] stands as the most sophisticated calculation of indirect optical absorption available today, yet it is not entirely parameter free since an empirical shift of the absorption onset at each temperature was needed in order to achieve agreement with experiment. This correction was unavoidable because the HBB theory does not take into account the temperature dependence of band structures.

A consistent theory of temperature-dependent band structures was developed by Allen and Heine (AH) [8,9]. In recent years this approach was successfully demonstrated and improved within the framework of first-principles density-functional theory calculations [10–13]. Given these recent advances it is natural to ask whether the HBB theory of indirect absorption and the AH theory of temperature-dependent band structures could be combined in a more general formalism, in view of fully predictive calculations of phonon-assisted optical processes at finite temperature.

In this manuscript we show that the quasiclassical method introduced by Williams [14] and Lax [15] (WL) provides a unified framework for calculating optical absorption spectra of solids, including phonon-assisted absorption and electron-phonon renormalization on the same footing. Indeed, we show that the HBB and AH theories can be derived from the WL formalism by neglecting electron-phonon scattering beyond one-phonon processes. In order to demonstrate the power of the WL approach we calculate from first principles the phonon-assisted optical absorption spectrum of silicon at different temperatures using a stochastic importance sampling Monte Carlo method [16] and no adjustable parameters. Our calculations are in very good agreement with experimental spectra measured at several temperatures. We also calculate temperature-dependent band gaps and find good agreement with experiment.

The premise of the conventional HBB theory is that electrons in solids experience a time-dependent potential which arises from the oscillatory motion of the atoms around their equilibrium positions. Following this premise, indirect electronic transitions are obtained within time-dependent perturbation theory to first order in the atomic displacements [4]. This amounts to considering optical transitions whereby the absorption of a photon is accompanied by the emission or absorption of one phonon.

At variance with the HBB point of view, in the WL approach electrons and phonons are described on the same footing, and optical excitations correspond to transitions between Born-Oppenheimer product states of electrons and quantum nuclei [14,15]. The quantized final vibrational states are then replaced by a classical continuum, leading to an expression for the optical absorption which only involves the nuclear wave function of the initial state [15]. This replacement can be justified using the adiabatic approximation. The temperature dependence is then obtained as a canonical average over the initial states of the system. This theory was successfully employed to explain the optical properties of cold lithium clusters [17] and diamondoids [16].

The imaginary part of the WL temperature-dependent dielectric function is given by

$$\epsilon_2(\omega; T) = Z^{-1} \sum_n \exp(-E_n/k_B T) \langle \epsilon_2(\omega; x) \rangle_n, \quad (1)$$

where ω is the photon frequency, k_B the Boltzmann constant, and T the temperature. Z is the canonical partition function among the quantum nuclear states with energies E_n, and $\langle \rangle_n$ stands for the expectation value taken over the nth many-body nuclear wave function. $\epsilon_2(\omega; x)$ denotes the imaginary part of the dielectric function evaluated with the nuclei clamped at the positions specified by the set of normal coordinates $\{x_\nu\}$, which we indicate collectively as x. In order to keep the notation light we label the normal modes of vibration and the electronic states by integer indices; accordingly, the following equations will refer to a Born–von Kármán (BvK) supercell of the crystal unit cell. An intuitive interpretation of Eq. (1) is that in the adiabatic approximation the electronic and nuclear time scales are decoupled, and the measured absorption spectrum is described as an ensemble average over instantaneous absorption spectra at fixed nuclear coordinates. In the harmonic approximation Eq. (1) simplifies via Mehler's formula [18]:

$$\epsilon_2(\omega; T) = \int \Pi_\nu dx_\nu G[x_\nu; \langle x_\nu^2 \rangle_T] \epsilon_2(\omega; x), \quad (2)$$

where $G[u; \sigma^2]$ is a normalized Gaussian of width σ in the variable u. $\langle x_\nu^2 \rangle_T = (2n_\nu + 1)l_\nu^2$ represents the mean square nuclear displacement at the temperature T, with n_ν the Bose-Einstein occupation factor of the mode with energy $\hbar\omega_\nu$ at the temperature T, and l_ν the corresponding zero-point amplitude [19].

For simplicity we calculate the dielectric function within the independent-particle approximation, although the present formalism is general and can be used with any description of optical transitions at fixed nuclei. In the electric dipole approximation we have [20]

$$\epsilon_2(\omega; x) = \frac{2\pi}{mN} \frac{\omega_p^2}{\omega^2} \sum_{cv} |p_{cv}^x|^2 \delta(\varepsilon_c^x - \varepsilon_v^x - \hbar\omega), \quad (3)$$

where m is the electron mass, ω_p the plasma frequency, N the number of electrons in the unit cell, and the factor of 2 is for the spin degeneracy. p_{cv}^x is the matrix element of the momentum operator along the polarization direction of the photon, taken between the valence and conduction Kohn-Sham states $|v^x\rangle$ and $|c^x\rangle$ with energies ε_v^x and ε_c^x, respectively. The superscripts indicate that these states are calculated with the nuclei fixed in the configuration specified by the normal coordinates x; the same quantities evaluated at the equilibrium atomic positions will be denoted without superscripts. Equation (2) was evaluated within density functional theory using importance sampling Monte Carlo integration in a BvK supercell, as described below in the Methods.

In Fig. 1(a) we compare the optical absorption coefficient of silicon calculated from first principles using Eqs. (2) and (3) with the experimental spectrum, both at 300 K. The absorption coefficient was obtained as $\kappa(\omega; T) = \omega\epsilon_2(\omega; T)/cn(\omega)$, where c is the speed of light and $n(\omega)$ the refractive index. The spectrum calculated with the nuclei clamped in their equilibrium positions [dashed blue line in Fig. 1(a)] exhibits an onset around 3.3 eV, corresponding to the direct $\Gamma_{25v}' \rightarrow \Gamma_{15c}$ transition in silicon. The subgap absorption between 1.1–3.3 eV observed in experiments [21] is completely missing in this calculation. At variance with this result, our WL spectrum correctly captures indirect absorption [solid blue line in Fig. 1(a)], and exhibits very good agreement with experiment without any adjustable parameters. Since we are not including excitonic effects, the strength of the E_1 transition is underestimated in our calculations, as can be seen at energies around 3.3 eV in Fig. 1(a) [22]. The agreement
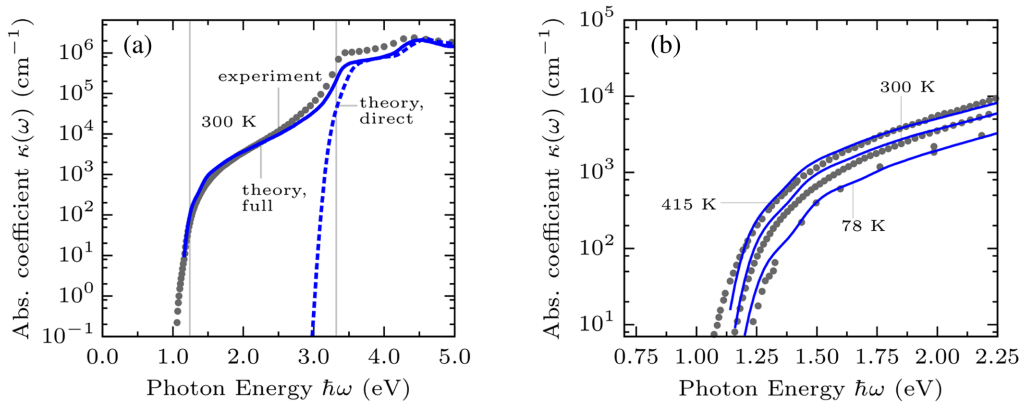

FIG. 1 (color online). (a) The absorption coefficient of bulk silicon at 300 K: calculation with the atoms clamped at their equilibrium positions (blue dashed line), calculation using the WL method [Eq. (2), blue solid line], and experimental data from Ref. [21] (gray filled discs). The thin vertical lines indicate the direct and indirect band gaps with nuclei in their equilibrium positions. (b) Temperature dependence of the absorption coefficient of silicon: WL theory (solid lines) and experimental data for 78 K [23], 300 K [21], and 415 K [24] (gray discs). The calculated spectra were broadened using Gaussians of width 30 meV, and truncated at the smallest excitation energy in order to avoid artifacts.

between theory and experiment in Fig. 1 remarkably extends over 5 orders of magnitude.

In order to shed light on the ability of the WL theory to capture indirect optical absorption we express the dependence of the optical matrix elements on the atomic positions using time-independent perturbation theory. To first order in the atomic displacements we have

$$p_{cv}^x = p_{cv} + \sum_{n\nu}' \left[\frac{p_{cn}g_{n\nu}}{\varepsilon_v - \varepsilon_n} + \frac{g_{cn\nu}p_{n\nu}}{\varepsilon_c - \varepsilon_n} \right] \frac{x_\nu}{l_\nu}, \qquad (4)$$

where $g_{mn\nu} = \langle m|\partial V/\partial x_\nu|n\rangle l_\nu$ is the electron-phonon matrix element associated with the Kohn-Sham potential V, and in the primed summation the terms $n = c$, v are skipped. The spectral range of indirect absorption corresponds to photon energies $\hbar\omega < E_g^d$, with $E_g^d = 3.3$ eV being the direct band gap of silicon. In this range direct optical transitions are forbidden; therefore, from Eq. (4) we have $p_{cv} = 0$. If we retain only one-phonon processes and neglect the dependence of the electron energies on the nuclear coordinates, Eqs. (2)–(4) yield

$$\epsilon_2(\omega; T) = \frac{2\pi}{mN} \frac{\omega_p^2}{\omega^2} \sum_{cv\nu} \left| \sum_n' \frac{p_{cn}g_{n\nu}}{\varepsilon_n - \varepsilon_v} + \frac{g_{cn\nu}p_{n\nu}}{\varepsilon_n - \varepsilon_v - \hbar\omega} \right|^2$$
$$\times \delta(\varepsilon_c - \varepsilon_v - \hbar\omega)(2n_\nu + 1). \qquad (5)$$

This expression is essentially the same as given by the conventional HBB theory of indirect optical absorption [4], and employed in the first-principles calculations of Ref. [5]. The only difference is that the HBB theory contains phonon energies $\pm\hbar\omega_\nu$ in the denominators and the Dirac delta functions, corresponding to phonon emission and absorption processes, respectively. In the WL approach these terms are neglected since in the adiabatic approximation $\hbar\omega_\nu \ll \varepsilon_c - \varepsilon_v$. In Fig. S1 [25] we show that the present result agrees well with the indirect absorption spectrum of silicon calculated using the conventional HBB theory in Ref. [5].

In Fig. 1(b) we compare our calculated temperature dependence of the indirect optical absorption line shape of silicon with experiment. We focus on the energy range 1.1–2.3 eV where the effect of excitonic spectral weight transfer on the dielectric function is negligible. Our calculations are in good agreement with experiment. In particular, the theoretical spectra capture both the smooth increase of the absorption coefficient with temperature, and the concurrent redshift of the absorption onset. We stress that the observed redshift arises naturally in our calculations, in contrast with the HBB theory where this effect needs to be included empirically [5]. The slight loss of intensity near the indirect edge at the highest temperature [spectrum at 415 K in Fig. 1(b)] results from the incomplete sampling of multiphonon processes in our stochastic approach.

In order to understand the effect of temperature in the WL approach we note that temperature enters the formalism in two ways: first, in the Bose-Einstein factors $(2n_\nu + 1)$ in Eq. (5), as in the conventional HBB theory. This term mainly modifies the absorption intensity. Second, temperature enters in the electron-phonon renormalization of the electronic band structure, leading to a temperature-dependent shift of the absorption onset. The latter contribution can be analyzed by rewriting the energies inside the Dirac delta functions in Eq. (3) using time-independent perturbation theory. The result, accurate to second order in the atomic displacements, reads

$$\varepsilon_c^x = \varepsilon_c + \sum_\nu g_{cc\nu} \frac{x_\nu}{l_\nu} + \sum_{\mu\nu} \left[\sum_n' \frac{g_{cn\mu}g_{nc\nu}}{\varepsilon_c - \varepsilon_n} + h_{c\mu\nu} \right] \frac{x_\mu x_\nu}{l_\mu l_\nu}, \qquad (6)$$

where $h_{n\mu\nu} = \langle n|\partial^2 V/\partial x_\mu \partial x_\nu|n\rangle l_\mu l_\nu/2$ is the Debye-Waller electron-phonon matrix element [8,9]. If we evaluate the average of ε_c^x in Eq. (6) following the same prescription as for the dielectric function in Eq. (2) we obtain (up to third order in the displacements)

$$\varepsilon_c(T) = \varepsilon_c + \sum_\nu \left[\sum_n' \frac{|g_{cn\nu}|^2}{\varepsilon_c - \varepsilon_n} + h_{c\nu\nu} \right] (2n_\nu + 1). \qquad (7)$$

In the first term inside the square brackets we recognize the Fan (or self-energy) electron-phonon renormalization; the second term is the Debye-Waller renormalization [6,8–10,12,13]. Both terms can be derived from a diagrammatic analysis by considering only one-phonon processes [27]. Equation (7) represents precisely the AH theory of temperature-dependent band structures, and explains the temperature shift of the indirect absorption line shapes in Fig. 1(b).

From the calculated optical absorption spectra we can extract the temperature dependence of the indirect and direct band gaps of silicon, following the standard *experimental* procedure. In fact, within the HBB theory the absorption coefficient near the indirect edge goes like $\omega^{-1}(\hbar\omega - E_g \pm \hbar\omega_\nu)^2$ [4,20]; therefore, the indirect gap E_g is straightforwardly extracted from a linear fit to $\omega^{1/2}\kappa(\omega)^{1/2}$. As expected, Fig. 2(a) shows that our calculated spectra follow a straight line when plotted as $\omega^{1/2}\kappa(\omega)^{1/2}$. The intercept of this line with the horizontal axis yields the indirect band gaps for each temperature, and the results are shown in Fig. 2(b) for two fitting ranges, 0–1.5 eV and 0–2 eV. Single-oscillator fits to our data using $E_g(T) = E_g(0) - a_B\{1 + 2/[\exp(\Theta/T) - 1]\}$ following Ref. [28] gave a zero-point renormalization of $a_B = 60$–72 meV and an effective temperature $\Theta = 368$–494 K for the two ranges considered. These values are in good agreement with the experimental data 62 meV and 395 K, respectively [29].

In Fig. S3 [25] we show that the WL spectrum can also be used to extract the temperature dependence of the *direct*
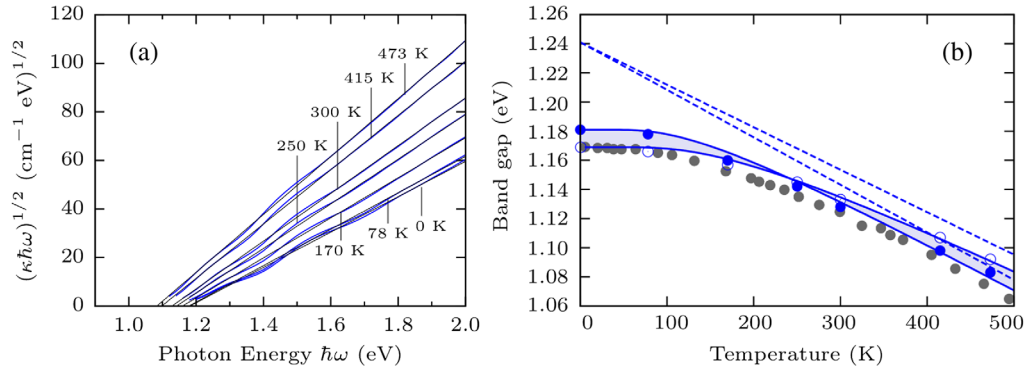
FIG. 2 (color online). (a) Extraction of the temperature-dependent indirect band gap of silicon using line shape analysis. The calculated $[\omega\kappa(\omega)]^{1/2}$ at each temperature are shown as blue lines, and the corresponding linear fits as thin black lines. The intercepts of the straight lines with the horizontal axis give the band gaps. The linear fits were determined in the energy range 0–2 eV. (b) Temperature-dependent indirect band gap of silicon: the band gaps extracted from the line shape analysis in (a) using linear fits in the ranges 0–2 eV and 0–1.5 eV are shown as blue filled discs and open circles, respectively. Gray filled discs are experimental data from Ref. [30]. The solid lines are single-oscillator fits to the calculated data, and the dashed lines are the corresponding high-temperature asymptotes. Figure S2 [25] shows the sensitivity of the band gaps to the fitting range. The shading is a guide to the eye and can be taken as the uncertainty of the theoretical band gaps.

band gap of silicon using standard line shape analysis of second-derivative spectra. Also in this case we obtain good agreement with experiment. Overall the agreement between theory and experiment in Figs. 1, 2, and Fig. S3 [25] provides strong support to the validity of the WL theory for first-principles calculations of phonon-assisted optical absorption spectra.

In future work it will be important to test the role of additional correction terms, such as nonadiabaticity [12], quasiparticle corrections [13], and anharmonicity [31]. While these further refinements will modify the precise values of the zero-point renormalization of the band gap, it is expected that they will not change any of the features of the line shapes in Fig. 1.

The stochastic approach employed here is remarkably efficient in sampling the vibrational phase space, to the point that the optical spectrum can be calculated using a *single configuration* of the nuclei (Fig. S4 [25]). This is an unexpected finding and warrants separate investigation. While the present method lacks the elegance of standard density-functional perturbation theory approaches [32], it comes with distinctive advantages: (i) the electron-phonon coupling is included to all orders, (ii) the method can be used in conjunction with higher-level theories, such as hybrid functionals [33,34] and the *GW* or Bethe-Salpeter method [35], and (iii) the anharmonicity of the potential energy surface can be incorporated by using the appropriate nuclear wave functions [36].

In conclusion, we have demonstrated a new theory of phonon-assisted optical absorption in solids, based on the Williams-Lax quasiclassical approximation. This theory incorporates for the first time the temperature-dependent electron-phonon renormalization of the electronic structure, and enables calculations of optical spectra at finite temperature over a wide spectral range. Our stochastic approach is

efficient and easy to implement on top of any electronic structure package. The present Letter opens the way to systematic calculations of optical spectra of semiconductors and insulators at finite temperature.

Methods.—The calculations were performed within density functional theory in the local density approximation [37,38], using plane-wave basis sets and norm-conserving pseudopotentials [39] as implemented in the Quantum ESPRESSO suite [40]. We obtained vibrational frequencies and eigenmodes via the frozen-phonon method [41,42]. The optical matrix elements including the nonlocal components of the pseudopotential [43] were evaluated using Yambo [44]. Calculations with or without the nonlocal components of the pseudopotential are compared in Fig. S1 [25]. In order to address the band-gap problem we used a scissor correction $\Delta = 0.75$ eV in all calculations, close to the *GW* value of Ref. [45]. The nonlocality of the scissor operator was taken into account in the oscillator strengths [43] via the renormalization factors $(\varepsilon_c - \varepsilon_v)/(\varepsilon_c - \varepsilon_v + \Delta)$, thereby ensuring that the f-sum rule be correctly fulfilled. A comparison between the absorption spectra calculated with or without the scissor correction is shown in Fig. S5 [25]. We averaged over atomic configurations using importance sampling Monte Carlo integration [16]. The estimator [46] of $\varepsilon_2(\omega; T)$ in Eq. (2) was obtained using configurations generated from a random set of normal coordinates $\{x_\nu\}$, as determined from the quantile function of the Gaussian distribution, $x_\nu = (2\langle x_\nu^2\rangle_T)^{1/2}\mathrm{erf}^{-1}(2t - 1)$ [47]. The t values (one for each normal coordinate, $0 < t < 1$) were generated via Sobol low-discrepancy sequences [48] by skipping the first 100 steps. We found that 5–8 atomic configurations are enough to converge the spectra at high or low temperature, respectively. Figure S4 [25] shows that even using a single configuration the spectrum is already

converged. The results presented in Figs. 1 and 2 were obtained using a $8 \times 8 \times 8$ BvK supercell of the silicon unit cell. We sampled the Brillouin zone of the supercell using 30 random points with weights determined by a Voronoi analysis [49]. Convergence tests with respect to the supercell size and Brillouin zone sampling are shown in Fig. S6 [25]. In Fig. 2(a) the spectrum was calculated using a Gaussian broadening of 30 meV; in Fig. S4(b) [25] we show that even when using a broadening of only 1 meV the spectra remain essentially unaltered. Figure S7 [25] shows that the variation of the band gap due to the thermal expansion of the lattice [26] is smaller than 5 meV up to 500 K, and can be neglected.

---

[*]Present address: Center for Atomic-Scale Materials Design (CAMD), Department of Physics, Technical University of Denmark, DK-2800 Kongens Lyngby, Denmark.

[†]feliciano.giustino@materials.ox.ac.uk

[1] C. Kittel, *Introduction to Solid State Physics*, 5th ed. (Wiley, New York, 1976).

[2] N. W. Ashcroft and N. D. Mermin, *Solid State Physics* (Harcourt College Publishers, New York, 1976).

[3] L. Hall, J. Bardeen, and F. Blatt, Phys. Rev. **95**, 559 (1954).

[4] F. Bassani and G. Pastori Parravicini, *Electronic States and Optical Transition in Solids* (Pergamon Press, Oxford, 1975).

[5] J. Noffsinger, E. Kioupakis, C. G. Van de Walle, S. G. Louie, and M. L. Cohen, Phys. Rev. Lett. **108**, 167402 (2012).

[6] F. Giustino, M. L. Cohen, and S. G. Louie, Phys. Rev. B **76**, 165108 (2007).

[7] N. Marzari, A. A. Mostofi, J. R. Yates, I. Souza, and D. Vanderbilt, Rev. Mod. Phys. **84**, 1419 (2012).

[8] P. B. Allen and V. Heine, J. Phys. C **9**, 2305 (1976).

[9] M. Cardona and M. L. W. Thewalt, Rev. Mod. Phys. **77**, 1173 (2005).

[10] A. Marini, Phys. Rev. Lett. **101**, 106405 (2008).

[11] F. Giustino, S. G. Louie, and M. L. Cohen, Phys. Rev. Lett. **105**, 265501 (2010).

[12] E. Cannuccia and A. Marini, Phys. Rev. Lett. **107**, 255501 (2011).

[13] G. Antonius, S. Poncé, P. Boulanger, M. Côté, and X. Gonze, Phys. Rev. Lett. **112**, 215501 (2014).

[14] F. E. Williams, Phys. Rev. **82**, 281 (1951).

[15] M. Lax, J. Chem. Phys. **20**, 1752 (1952).

[16] C. E. Patrick and F. Giustino, Nat. Commun. **4**, 2006 (2013).

[17] F. Della Sala, R. Rousseau, A. Görling, and D. Marx, Phys. Rev. Lett. **92**, 183401 (2004).

[18] G. N. Watson, J. Lond. Math. Soc. **s1-8**, 194 (1933).

[19] C. E. Patrick and F. Giustino, J. Phys. Condens. Matter **26**, 365503 (2014).

[20] P. Y. Yu and M. Cardona, *Fundamentals of Semiconductors*, 4th ed. (Springer, Heidelberg, 2010), pp. 200–343.

[21] M. A. Green and M. J. Keevers, Prog. Photovoltaics **3**, 189 (1995).

[22] L. X. Benedict, E. L. Shirley, and R. B. Bohn, Phys. Rev. B **57**, R9385 (1998).

[23] R. Braunstein, M. R. Arnold, and F. Herman, Phys. Rev. **109**, 695 (1958).

[24] H. A. Weakliem and D. Redfield, J. Appl. Phys. **50**, 1491 (1979).

[25] See Supplemental Material at http://link.aps.org/supplemental/10.1103/PhysRevLett.115.177401 for Supplemental Figs. S1–S7, and Supplemental Ref. [26].

[26] Y. Okada and Y. Tokumaru, J. Appl. Phys. **56**, 314 (1984).

[27] A. Marini, S. Poncé, and X. Gonze, Phys. Rev. B **91**, 224310 (2015).

[28] P. Lautenschlager, M. Garriga, L. Vina, and M. Cardona, Phys. Rev. B **36**, 4821 (1987).

[29] M. Cardona, Solid State Commun. **133**, 3 (2005).

[30] V. Alex, S. Finkbeiner, and J. Weber, J. Appl. Phys. **79**, 6943 (1996).

[31] I. Errea, M. Calandra, and F. Mauri, Phys. Rev. B **89**, 064302 (2014).

[32] S. Baroni, S. de Gironcoli, A. Dal Corso, and P. Giannozzi, Rev. Mod. Phys. **73**, 515 (2001).

[33] J. P. Perdew, M. Ernzerhof, and K. Burke, J. Chem. Phys. **105**, 9982 (1996).

[34] J. Heyd, G. E. Scuseria, and M. Ernzerhof, J. Chem. Phys. **118**, 8207 (2003).

[35] G. Onida, L. Reining, and A. Rubio, Rev. Mod. Phys. **74**, 601 (2002).

[36] B. Monserrat, N. D. Drummond, and R. J. Needs, Phys. Rev. B **87**, 144302 (2013).

[37] D. M. Ceperley and B. J. Alder, Phys. Rev. Lett. **45**, 566 (1980).

[38] J. P. Perdew and A. Zunger, Phys. Rev. B **23**, 5048 (1981).

[39] M. Fuchs and M. Scheffler, Comput. Phys. Commun. **119**, 67 (1999).

[40] P. Giannozzi et al., J. Phys. Condens. Matter **21**, 395502 (2009).

[41] K. Kunc and R. M. Martin, in *Ab Initio Calculation of Phonon Spectra*, edited by J. Devreese, V. Van Doren, and P. Van Camp (Plenum, New York, 1983), p. 65.

[42] G. J. Ackland, M. C. Warren, and S. J. Clark, J. Phys. Condens. Matter **9**, 7861 (1997).

[43] A. F. Starace, Phys. Rev. A **3**, 1242 (1971).

[44] A. Marini, C. Hogan, M. Grüning, and D. Varsano, Comput. Phys. Commun. **180**, 1392 (2009).

[45] H. Lambert and F. Giustino, Phys. Rev. B **88**, 075117 (2013).

[46] R. E. Caflisch, Acta Numer. **7**, 1 (1998).

[47] S. E. Brown, I. Georgescu, and V. A. Mandelshtam, J. Chem. Phys. **138**, 044317 (2013).

[48] S. Joe and F. Y. Kuo, SIAM J. Sci. Comput. **30**, 2635 (2008).

[49] F. Aurenhammer, ACM Comput. Surv. **23**, 345 (1991).